

V440 Per: the longest-period overtone Cepheid

R. Baranowski,¹* R. Smolec,² W. Dimitrov,¹ T. Kwiatkowski,¹
 A. Schwarzenberg-Czerny,^{1,2}† P. Bartczak,¹ M. Fagas,¹ W. Borczyk,¹ K. Kamiński,¹
 P. Moskalik,² R. Ratajczak¹ and A. Rożek¹

¹*Astronomical Observatory of Adam Mickiewicz University, ul. Słoneczna 36, PL 60-286 Poznań, Poland*

²*Copernicus Astronomical Centre, ul. Bartycka 18, PL 00-716 Warsaw, Poland*

Accepted 2009 April 3. Received 2009 April 1; in original form 2009 January 17

ABSTRACT

V440 Per is a Population I Cepheid with a period of 7.57 d and low-amplitude, almost sinusoidal light and radial velocity curves. With no reliable data on the first harmonic, its pulsation mode identification remained controversial. We obtained a radial velocity curve of V440 Per with our new high-precision and high-throughput Poznań Spectroscopic Telescope. Our data reach an accuracy of 130 m s^{-1} per individual measurement and yield a secure detection of the first harmonic with an amplitude of $A_2 = 140 \pm 15 \text{ m s}^{-1}$. The velocity Fourier phase ϕ_{21} of V440 Per is inconsistent at the 7.25σ level with those of fundamental-mode Cepheids, implying that the star must be an overtone Cepheid, as originally proposed by Kienzle et al. Thus, V440 Per becomes the longest-period Cepheid with securely established overtone pulsations. We show that a convective non-linear pulsation hydrocode can reproduce the Fourier parameters of V440 Per very well. The requirement to match the observed properties of V440 Per constrains the free parameters of the dynamical convection model used in the pulsation calculations, in particular the radiative loss parameter.

Key words: hydrodynamics – methods: data analysis – techniques: spectroscopic – stars: individual: V440 Per – stars: oscillations – Cepheids.

1 INTRODUCTION

The Population I *sinusoidal* or s-Cepheids are a small group of Cepheids pulsating in the first radial overtone. In the Galaxy, where individual Cepheid distances are usually not accurately known, the s-Cepheids are discriminated from the fundamental-mode pulsators by the Fourier decomposition of their light curves (Antonello, Poretti & Reduzzi 1990). The method works well only for variables with periods below 5 d. Fortunately, it can be extended to longer periods with the help of the radial velocity curves, as was shown by Kienzle et al. (1999). Studies of longer-period overtone Cepheids are of great interest. The velocity Fourier parameters of s-Cepheids display a very characteristic progression with period, which is attributed to the 2:1 resonance at $P = 4.2\text{--}4.6$ d between the first and fourth overtones (Kienzle et al. 1999; Feuchtinger, Buchler & Kolláth 2000). Unfortunately, any detailed modelling of this progression and pinpointing of the resonance position is hampered by a scarcity of s-Cepheids with $P > 5.5$ d, with MY Pup being the only secure identification. One more candidate, V440 Per ($P = 7.57$ d), has been identified by Kienzle et al. (1999). They noted that the velocity Fourier phase ϕ_{21} places this Cepheid away from the

fundamental-mode sequence and possibly on to the first-overtone sequence. On this basis, Kienzle et al. (1999) proposed that V440 Per is an overtone pulsator. This hypothesis was further supported by determination of the phase lag between the light curve and the radial velocity curve, $\Delta\Phi_1 = \phi_1^{Vr} - \phi_1^{\text{mag}}$, which also placed V440 Per away from the fundamental sequence (Ogłóza, Moskalik & Kanbur 2000). However, V440 Per is a small-amplitude, nearly sinusoidal variable. Even the best radial velocity data then available (Burki & Benz 1982) yielded large errors of the first-harmonic Fourier parameters; the measurement error of the phase lag $\Delta\Phi_1$ was also large. This, and inconsistency with their hydrodynamic pulsation models, led Szabó, Buchler & Bartee (2007) to dispute the mode identification of V440 Per. They noted that the membership of this Cepheid in the fundamental-mode sequence could not be rejected at the 3σ confidence level. They argued that V440 Per is not an overtone pulsator, but rather a fundamental-mode Cepheid of very low amplitude.

In the present paper we report the results of an extensive campaign of observations of V440 Per with the Poznań Spectroscopic Telescope, lasting almost a year and aimed at obtaining high-quality data suitable for detailed diagnostics and comparison with non-linear models. In Section 2 we describe our instrument and observations. In Section 3 we discuss the quality of our radial velocities and derive the Fourier parameters of V440 Per. A comparison with the Fourier parameters of other Galactic Cepheids and the

*Based on observations from Poznań Spectroscopic Telescope

†E-mail: alex@camk.edu.pl

identification of the pulsation mode of V440 Per is discussed in Section 4. In Section 5 we perform a detailed comparison of V440 Per with non-linear overtone Cepheid models. Our conclusions are summarized in Section 6.

2 OBSERVATIONS AND DATA REDUCTION

Our observations were obtained with the new Poznań Spectroscopic Telescope (PST) of Adam Mickiewicz University. Its full description is not published yet, hence we devote some space here to an instrument description and data-quality evaluation.

2.1 Poznań Spectroscopic Telescope

The PST is located in Poland at the Borowiec station, 20 km south from Poznań city, at a meagre elevation of 123 m above sea level. The PST consists of parallel twin 0.4-m Newton telescopes of the f ratio 4.5, fixed on a single parallactic fork mount. An acquisition box at the Newton focus of each telescope holds the tip of the fibre feeding our spectrograph, the thorium/argon (Th/Ar) calibration lamp and the autoguider camera SBIG ST-7.

Via a fibre the telescope feeds an Echelle spectrograph, a clone of the MUlti SIte COntinuous Spectroscopy (MUSICOS) design (Baudrand & Bohm 1992), red arm only. Our spectra are recorded with the low-noise Andor DZ436 camera fitted with a $2k \times 2k$ E2V 42–40 back-illuminated CCD chip, cooled with Peltier cells. About 60 orders are recorded, covering a spectral range of 4480–9250 Å at the inverse resolution of $\lambda/\delta\lambda = 35\,000$. The spectrograph is located in a thermo-isolated enclosure in the telescope dome. The sliding-roof dome, the telescope and its spectrograph all operate under full computer control. A full description of our instrumentation will be published elsewhere. Our system is operated interactively from the terminal. Such an operation mode does not compromise our data quality but requires an excessive workload. A substantial software effort is needed to achieve fully robotic operation.

2.2 Data pipeline

Routine CCD reductions up to spectra extraction, wavelength calibration and velocity measurement are performed using IRAF tasks combined into our reduction pipeline. Velocities are measured by cross-correlation, using the IRAF FXCOR task. The internal error estimates from FXCOR, of the order of a few km s^{-1} , relate to the line width and not to the actual measurement precision. They may serve for weighting purposes, however. So far, we have employed no standard star calibrations and our velocities are measured solely with respect to the Th/Ar lamp. For short-span observations such a primitive procedure still yields root-mean-square (RMS) residuals in the 100–200 m s^{-1} range, for stars brighter than 11 mag. As demonstrated in Section 3, for intensively observed, strictly periodic stars any long-term effects of a floating instrumental zero-point may be removed with some assurance, again yielding RMS residuals smaller than 150 m s^{-1} , over a one-year span of data.

2.3 Observations

In total 158 radial velocity measurements of V440 Per were obtained with the PST from 2007 August 15 to 2008 July 03. To reach a signal-to-noise ratio of 70 we exposed spectra for 10–15 min and up to several spectra were obtained per night. The observed velocities are listed in Table 1, which is published in full in online version of this article. Phase-folded data with fitted Fourier series (Section 3)

Table 1. PST radial velocities of V440 Per. This is a sample of the full table, which is available in the online version of the paper (see Supporting Information).

MJD	$\Delta v_r^{(a)}$	$\Delta v_{r,\text{corr}}^{(b)}$
54327.0490	−0.61	−0.52
54332.0517	3.04	3.14
54332.0683	2.96	3.06
...
54649.0009	2.28	2.12
54650.9302	2.75	2.57
54650.9419	2.76	2.58

(a) Zero-shifted by about $-26.3 \pm 0.2 \text{ km s}^{-1}$.

(b) Corrected for instrumental effects (see text).

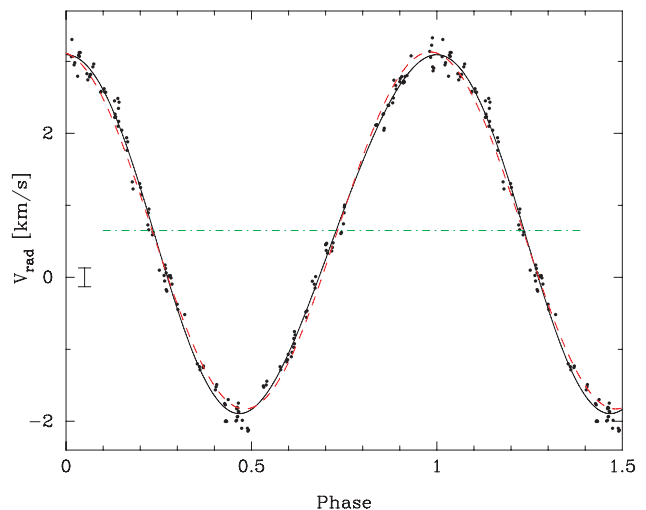


Figure 1. Radial velocities of V440 Per versus phase. First- and second-order Fourier fits are plotted with dashed and solid lines, respectively. The error bar indicates the ± 1 standard deviation of residuals. The velocities are corrected for small instrumental effects (see text). The zero-point is arbitrary.

are displayed in Fig. 1. In Fig. 2 we plot residuals of the first-order and second-order fits versus pulsation phase and time. Inspection of the plots demonstrates that our coverage was reasonably uniform, both in time and in frequency. From the residuals we estimate the standard error of our individual measurements as 130 m s^{-1} .

3 FOURIER PARAMETERS

The plot of the phase-folded radial velocities reveals near-sinusoidal variations with a peak-to-peak amplitude of 5 km s^{-1} . Some data consistency checks are due prior to drawing any final conclusions. Cepheid phases and frequencies are known to vary slightly. Additionally, the instrument stability over nine months needs checking. A preliminary non-linear least-squares fit of our data with a Fourier series of three harmonic terms (third-order fit) yielded no significant second harmonics of the main frequency or the period derivative term. Our fitted frequency of $0.13206 \pm 0.00001 \text{ c/d}$ is less accurate, yet consistent within the errors with the frequency derived by combining our data with the earlier measurements of Burki & Benz (1982), Arellano Ferro (1984) and Gorynya et al. (1992, 1996, 1998). Comparison of the data shows that the weighted zero-point shift of our velocities with respect to the previous authors is $-26.3 \pm 0.2 \text{ km s}^{-1}$.

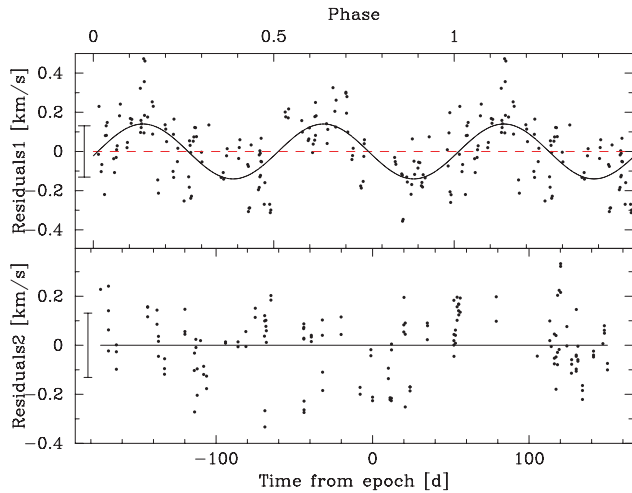


Figure 2. Upper panel: residuals of the first-order Fourier fit of V440 Per radial velocities (dashed line in Fig. 1) versus phase. The first harmonic is very small ($A_2 = 140 \pm 15 \text{ m s}^{-1}$), yet clearly visible. Lower panel: residuals of the second-order Fourier fit versus time.

Table 2. Fourier parameters of the V440 Per radial velocity curve.

Name	Value	Error	Unit
T_0	54498.783	0.008	MJD
P	7.5721	0.0006	d
A_1	2.480	0.015	km s^{-1}
A_2	0.140	0.015	km s^{-1}
R_{21}	0.056	0.006	1
ϕ_{21}	2.759	0.117	rad

The RMS deviation from the Fourier fit of all our data was 164 m s^{-1} , well in excess of the value of 135 m s^{-1} obtained for the first part of the data set. Worse, inspection of the residuals plotted against time sometimes revealed a non-Gaussian, bimodal distribution. The origin of both effects seems to be instrumental. To confirm that, we expanded our Fourier model by including two linear terms proportional to the time interval from the mid-epoch and to the hour angle of the star at the moment of observation. The fitted values of these instrumental correction coefficients were significant at 6σ and 5σ levels, respectively. From the overall covariance matrix we find a maximum absolute value of the correlation coefficients of 0.30, consistent with little interference between different fitted terms. These instrumental corrections reached up to $\pm 100 \text{ m s}^{-1}$. At this stage, we have no explanation for these corrections.

Our final second-order Fourier fit, supplemented with the instrumental correction terms, yielded a RMS deviation of 130 m s^{-1} , consistent with that obtained from the short-span observations. The values of the Fourier parameters of the V440 Per radial velocity curve are listed in Table 2 (for exact formulae defining the Fourier parameters and their errors see Appendix A).

4 PULSATION MODE OF V440 PER

The pulsation mode of a Cepheid can be established by measuring the Fourier phase ϕ_{21} of its light curve (Antonello et al. 1990) or radial velocity curve (Kienzle et al. 1999). This Fourier parameter does not depend on the pulsation amplitude of the star and for each mode it follows a different, *tightly defined* progression with the

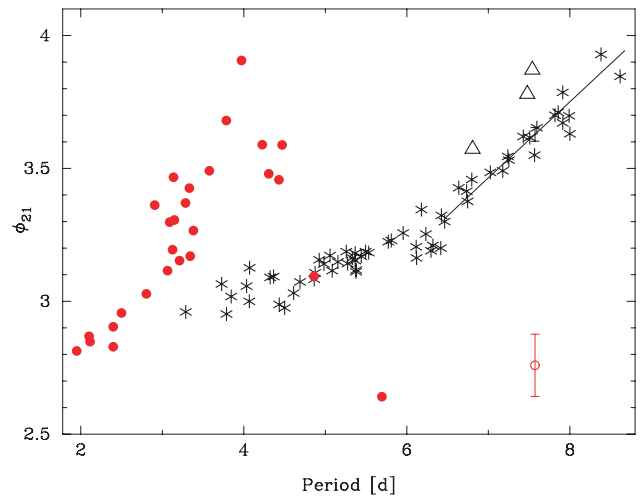


Figure 3. Fourier phase ϕ_{21} versus pulsation period for Cepheid radial velocity curves. Fundamental-mode Cepheids are marked with asterisks, except for low-amplitude ones ($A_1 < 10 \text{ km s}^{-1}$) which are marked with open triangles. Overtone Cepheids are denoted by filled circles. Observational data points are taken from Kienzle et al. (1999) and Moskalik, Gorynya & Samus (2009). The straight line indicates the best fit to the segment of the fundamental-mode progression. V440 Per is marked with an open circle.

pulsation period. For periods at which the two ϕ_{21} progressions are well separated, a secure mode identification can be achieved.

In Fig. 3 we plot the velocity ϕ_{21} of short-period Galactic Cepheids against their pulsation period P . Fundamental-mode pulsators and overtone pulsators are displayed with different symbols. V440 Per is plotted with an open circle. It is immediately obvious that it is located far apart from the fundamental-mode progression. This notion can be expressed using a quantitative basis. We selected a sample of 23 fundamental-mode Cepheids with periods P in the range $P_0 \pm 1.1 \text{ d}$, where $P_0 = 7.5721 \text{ d}$ is the period of V440 Per. To this sample we fitted a straight line $\phi_{21}(P) = a(P - P_0) + b$. With this procedure, we find that at the period of V440 Per the expected ϕ_{21} of the fundamental-mode Cepheid is 3.628 rad , with the average scatter of individual values of $\sigma_0 = 0.026 \text{ rad}$. This estimate of the intrinsic scatter is conservative, as the nominal ϕ_{21} measurement errors would account for at least half of it. The ϕ_{21} value measured for V440 Per is 2.759 rad , with an error of $\sigma_1 = 0.117 \text{ rad}$. The probability distribution of the ϕ_{21} offset, Δ , is obtained by convolution of two normal distributions, $N(0, \sigma_0)$ and $N(\Delta, \sigma_1)$. It may be demonstrated that the result is another normal distribution $N(\Delta, \sqrt{\sigma_0^2 + \sigma_1^2})$, essentially by virtue of the law of error combination. By substituting $\Delta = 3.628 - 2.759 = 0.869 \text{ rad}$, we find that the observed velocity ϕ_{21} of V440 Per deviates from the fundamental-mode sequence by 7.25σ . Thus, from purely observational evidence we conclude that V440 Per does not pulsate in the fundamental mode. Consequently, it must be an overtone Cepheid.

The argument presented above depends critically on the assumption that the velocity ϕ_{21} (at a given period) does not depend on the pulsation amplitude, which is lower for V440 Per than for the fundamental-mode Cepheids used as comparison. Such an assumption is well supported by numerical computations (Buchler, Moskalik & Kovács 1990; Smolec & Moskalik 2008); nevertheless it should be verified with available data. In Fig. 4 we plot residuals from the mean fundamental mode P - ϕ_{21} relation versus amplitude A_1 . In this case the mean relation is defined as the parabola fitted to all fundamental-mode Cepheids displayed in Fig. 3. For A_1 in the range 10 – 17 km s^{-1} there is no correlation of ϕ_{21} residuals with

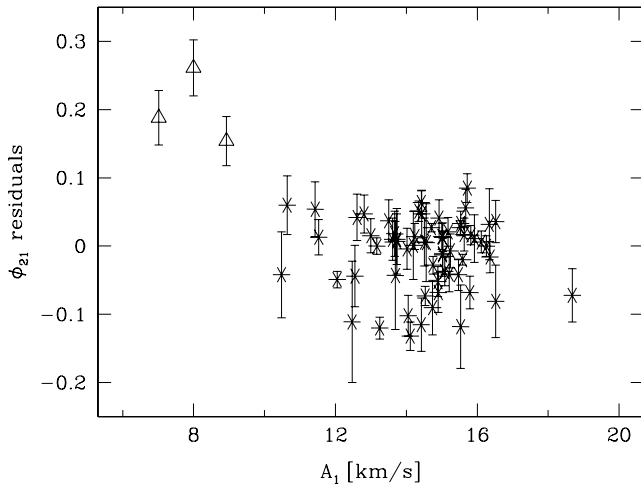


Figure 4. Residuals from the mean fundamental-mode P – ϕ_{21} relation versus pulsation amplitude A_1 . Observational data points are taken from Kienzle et al. (1999) and Moskalik et al. (2009). Symbols are the same as in Fig. 3.

pulsation amplitude. For $A_1 < 10 \text{ km s}^{-1}$ there is weak evidence of a ϕ_{21} increase. As the data are very scarce, we are not convinced that this increase is significant. If it were real, however, it would only strengthen our conclusion that V440 Per deviates strongly from the fundamental-mode sequence.

5 MODELLING OF V440 PER

Classification of V440 Per as a first-overtone pulsator, discussed in the previous section, is based solely on the morphological properties of Cepheid velocity curves. This mode identification can be strengthened by comparing the velocity curve of V440 Per with those of hydrodynamical Cepheid models. Such a comparison was first performed by Kienzle et al. (1999), who used the unpublished radiative models of Schaller & Buchler (private communication). They showed that the theoretical progression of velocity ϕ_{21} supported the overtone classification of V440 Per. However, their conclusion was somewhat weakened by a large error in the ϕ_{21} then available for this star.

In the present section, we confirm and extend the results of Kienzle et al. (1999). It is easy to show that the velocity curve of V440 Per is incompatible with fundamental-mode Cepheid models. Indeed, all published models display a velocity ϕ_{21} higher than 3.0 rad at *all periods* and higher than 3.5 rad at the period of V440 Per (Buchler, Moskalik & Kovács 1990; Moskalik, Buchler & Marom 1992; Smolec & Moskalik 2008). This holds true for both the convective models and the older radiative models. The computed velocity ϕ_{21} is very robust and shows no sensitivity to the treatment of convection, choice of opacities or details of the numerical code. Most importantly, it is insensitive to the pulsation amplitude (cf. figs 8, 11 of Smolec & Moskalik 2008). Clearly, the only chance to match the observed velocity curve of V440 Per is to search for an appropriate overtone model.

With this goal in mind, we computed several sequences of convective-overtone Cepheid models. We show that V440 Per fits the theoretical ϕ_{21} progression of first-overtone Cepheids and that its velocity Fourier parameters can be accurately reproduced with hydrodynamical computations.

Modelling such a long-period overtone pulsator is not an easy task. Satisfactory models have to reproduce Fourier parameters and the long period of this variable. The current hydrocodes used for

Table 3. Convective parameters of the pulsation models discussed in this paper. α_s , α_c , α_d , α_p and γ_r are given in units of standard values (see Smolec & Moskalik 2008). In the last column we give a linear upper limit for the first-overtone period (P_{max}).

Set	α	α_m	α_s	α_c	α_d	α_p	α_t	γ_r	P_{max} (d)
A	1.5	0.1	1.0	1.0	1.0	0.0	0.00	0.0	8.1
B	1.5	0.5	1.0	1.0	1.0	0.0	0.00	1.0	8.6
C	1.5	0.1	1.0	1.0	1.0	1.0	0.01	0.0	13.5

modelling of radial pulsations adopt time-dependent convection models (e.g. Stellingwerf 1982; Kuhfuß 1986). These models introduce several dimensionless parameters, which should be adjusted to match the observational constraints. V440 Per with its exceptionally long period offers an opportunity to impose interesting limits on the free parameters of the convection treatment.

In our computations we use the convective hydrocode of Smolec & Moskalik (2008). The code adopts the Kuhfuß (1986) dynamical convection model reformulated for use in stellar pulsation calculations. The Kuhfuß model is physically well motivated and self-consistent. It contains eight scaling parameters, a summary of which, together with a detailed description of the model equations, is provided by Smolec & Moskalik (2008). The values of the parameters used in the present paper are given in Table 3. All our Cepheid models are constructed in the way described in Smolec & Moskalik (2008). In all computations we use Galactic chemical composition ($X = 0.70$, $Z = 0.02$) and OPAL opacities (Iglesias & Rogers 1996) computed with the Grevesse & Noels (1993) mixture. We use the mass–luminosity (M – L) relation derived from Schaller et al. (1992) evolutionary tracks [$\log(L/L_{\odot}) = 3.56 \log(M/M_{\odot}) + 0.79$].

5.1 Pulsation period of V440 Per

Theoretical instability strips (IS) computed with the linear pulsation code for set A of the convective parameters are presented in Fig. 5. Instability strips for the first overtone and for the fundamental mode are enclosed with thick and thin lines, respectively. The dotted lines correspond to constant values of the first-overtone period, as indicated in the figure.

The first-overtone IS does not extend toward an arbitrarily high luminosity. The linear computations yield an upper limit for the first-overtone pulsation period, reaching $\sim 8.1 \text{ d}$ in Fig. 5 (see also Table 3). This limit depends mostly on the adopted convective parameters, but also on the M – L relation and the metallicity. However, to find a model that satisfies the V440 Per period constraint it is not enough to assure an appropriate linear period limit ($P > 7.5 \text{ d}$). This is because the maximum overtone period at *full-amplitude pulsation* is determined by non-linear effects.

Between the linear blue edges of the first overtone and the fundamental mode and below their crossing point, first-overtone pulsation is the only possibility. As one can see in Fig. 5, such a region is very narrow. A significant part of the overtone IS lies inside the fundamental-mode IS. For higher luminosity and overtone periods longer than 6 d , the instability strips of both modes entirely overlap.

In the region in which both modes are linearly unstable, the final pulsation state is determined by non-linear effects (modal selection). Full-amplitude pulsation in one of the modes usually suffices to saturate the instability. In principle, a double-mode pulsation is also possible, but it is very unlikely at the long overtone periods that are of interest in this paper (no double-mode pulsator with such a

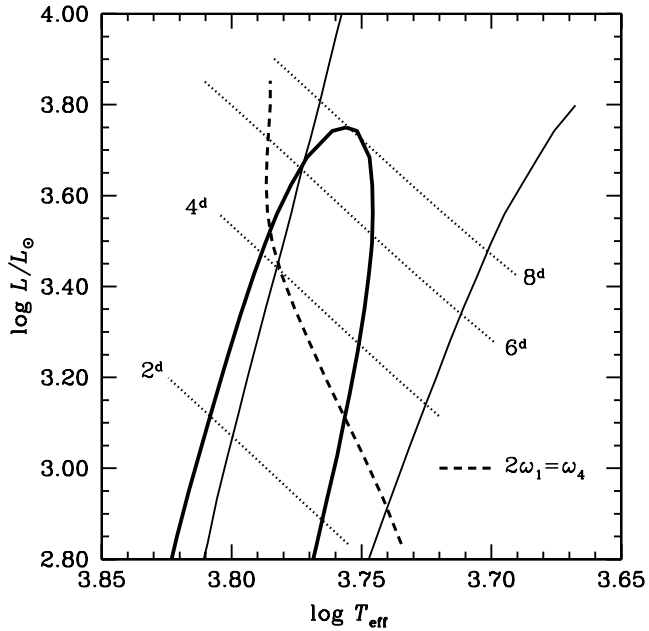


Figure 5. Theoretical instability strips for the convective parameters of set A.

long overtone period is known in either the Galaxy or the Magellanic Clouds: see Soszyński et al. 2008; Moskalik & Kołaczowski 2008). Therefore, construction of models matching the period of V440 Per requires both linear and non-linear computations and can be used to constrain the parameters of the convection model we use.

It is hard to constrain all eight parameters entering the model. As was shown by Yecko, Kolláth & Buchler (1998), different combinations of the convective α parameters may yield essentially the same results. Therefore we decided to freeze four parameters for which standard values are in use. In all studied sets of the convective parameters (Table 3), the mixing length is set to $\alpha = 1.5$ and for α_s , α_c and α_d we use the standard values (see Smolec & Moskalik 2008 for details). Set A represents the simplest convection model, without turbulent pressure, turbulent flux or radiative losses. These effects are turned on in set B (radiative losses) and in set C (turbulent pressure and turbulent flux). One of the crucial factors of the convection model is eddy-viscous damping, the strength of which is determined by the α_m parameter. The lower the eddy-viscous damping (the lower α_m), the more linearly unstable the models become and, consequently, the higher their pulsation amplitudes.

The most interesting outcome of the linear computations is the period limits, P_{\max} , given in the last column of Table 3. At the linear theory level, all sets of convective parameters listed in the table can satisfy the V440 Per period constraint. This was assured by adjusting the eddy-viscous damping parameter, α_m . In the case of sets A and C (no radiative losses), low values of α_m are required.

For each parameter set we computed a sequence of non-linear models, running parallel to the first-overtone blue edge, at a constant distance ΔT . In this section we use $\Delta T = 75$ K. This choice is arbitrary, but we believe that such models should reproduce most of the observed first-overtone variables. The static models were initialized in the first-overtone mode (as described in Smolec & Moskalik 2008) and their time evolution was followed until the final pulsation state was reached. The computed radial velocity curves were then decomposed into Fourier series. In Fig. 6 we plot amplitude A_1 versus pulsation period for three sequences of models. The most satisfactory results are obtained for set B of the convective param-

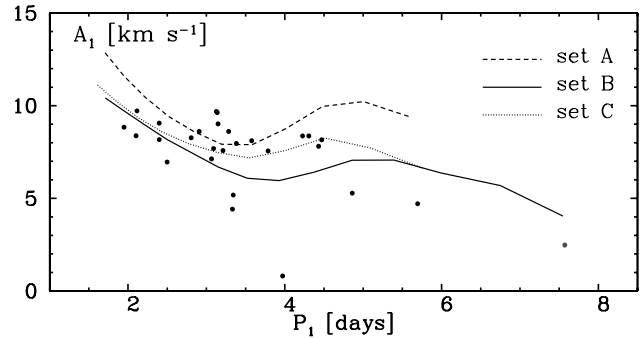


Figure 6. Fourier amplitude A_1 for three sequences of overtone Cepheid models. Model amplitudes are scaled by a constant projection factor of 1.4. Except for V440 Per, observational data points are taken from Kienzle et al. (1999) and Moskalik, Gorynya & Samus (in preparation).

eters. The pulsation amplitudes for this sequence are moderate and they match the observations well (this conclusion will be strengthened in Section 5.2). Also, for this sequence we obtain the overtone models with the longest periods. Sequences computed with the parameter sets A and C extend to periods not exceeding 6 d. All more massive models (i.e. with longer overtone periods) switched into the fundamental-mode pulsation and therefore are not plotted in the figure. The amplitudes of the models computed with the parameter sets A and C are larger. This is due to the adopted low value of eddy-viscous damping, needed to obtain a high enough limit for the linear overtone period. Any further decrease of α_m does not help. Although P_{\max} increases, models switch into the fundamental mode at periods well below the 7.57 d required to match V440 Per. Additionally, at short periods the amplitudes of the first-overtone models become unacceptably high. We conclude that inclusion of radiative losses is necessary to reproduce the long overtone period of V440 Per. As we will demonstrate in Section 5.2, with set B of the convective parameters we can also reproduce the Fourier parameters of V440 Per, as well as the overall progression of Fourier parameters for all observed overtone Cepheids.

Our conclusion is consistent with the results of Szabó et al. (2007). For convection with radiative losses,¹ their models extend toward high overtone periods (parameter set A of Szabó et al. 2007). Without radiative losses (set B of Szabó et al. 2007) and with much higher eddy-viscous dissipation than in our set A, their longest overtone periods fall below 3 d. Comparing our models with the overtone Cepheid models of Feuchtinger et al. (2000) we note some inconsistency. Feuchtinger et al. (2000) obtain long overtone periods for all sets of convective parameters considered in their paper. Their results are inconsistent with the results of Szabó et al. (2007) (set A of Feuchtinger et al. 2000 and set B of Szabó et al. 2007 are identical, but their linear results are significantly different) as well as with our results. We trace this discrepancy to a different evaluation of the superadiabatic gradient, $Y = \nabla - \nabla_a$, in our computations and in the Vienna code used by Feuchtinger et al. (2000). In the Vienna code, the radiative pressure contribution is neglected in the computation of ∇_a (Feuchtinger 1999). This leads to higher values of ∇_a (≈ 0.4 far from partial ionization regions, see figs 3 and 4 of Wuchterl & Feuchtinger 1998) and lower values of the superadiabatic gradient. Consequently, in their models convection

¹ Note, however, that in the Florida-Budapest hydrocode used by Szabó et al. (2007), radiative losses are modelled in a different way (see also Smolec & Moskalik 2008).

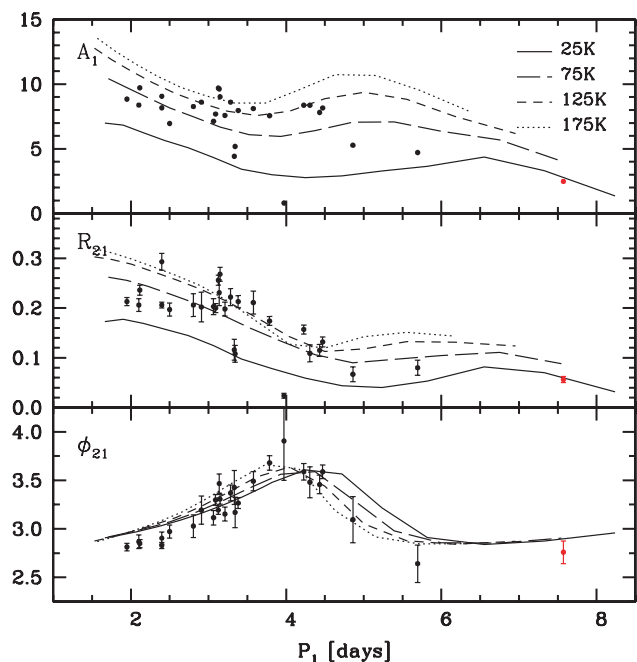


Figure 7. Fourier parameters of Cepheid radial velocity curves. Model sequences are computed at constant distances from the first-overtone blue edge, as indicated in the figure. Except for V440 Per, observational data points are taken from Kienzle et al. (1999) and Moskalik et al. (2009). Error bars for most of the amplitudes are smaller than the symbol size and are not plotted.

is less pronounced and the models are more unstable. In fact, we were able to reproduce their linear results when we neglected the contribution of radiation in the evaluation of ∇_a .

5.2 Fourier parameters of V440 Per

In this section we focus our attention on set B of the convective parameters. As demonstrated in the previous section, this parameter set allows us to reproduce long overtone periods and the observed pulsation amplitudes. In Fig. 7 we compare the velocity Fourier parameters of Galactic overtone Cepheids with those of the hydrodynamical models computed with the parameters of set B. Four sequences of models are displayed in the plot, run at different distances from the first-overtone blue edge ($\Delta T = 25, 75, 125, 175$ K). The overall observed progression of Fourier parameters is well reproduced with our models. For ϕ_{21} , we notice that the model sequences are shifted toward somewhat shorter periods. This can be easily explained. The characteristic progression of velocity ϕ_{21} with period is caused by the 2:1 resonance between the first overtone and the fourth overtone (Kienzle et al. 1999; Feuchtinger et al. 2000). The centre of this resonance is located at $P = 4.2\text{--}4.6$ d. The exact location of the resonance in hydrodynamic models depends mostly on the chosen mass–luminosity relation. This relation was not adjusted in our calculations to match the observed resonance progression.² As shown in Fig. 5, the resonance centre (dashed line) crosses the centre of the first-overtone IS for periods shorter than

² Adjustment of the M – L relation to satisfy the resonance constraint is not an easy task. Both the slope and the zero-point of the adopted M – L relation affect location of the resonance and the shape of the ϕ_{21} progression. In a forthcoming publication (Smolec & Moskalik, in preparation) we address this problem in detail.

4 d, which explains the horizontal shift in Fig. 7. Taking into account this shift, amplitudes, amplitude ratios and Fourier phases agree satisfactorily with observations, although at short periods theoretical ϕ_{21} values are slightly too high. Considering V440 Per, we see a very good agreement with the model sequence closest to the blue edge of the overtone instability strip ($\Delta T = 25$ K). An exact match can be easily obtained for a model sequence located slightly closer to the blue edge. We note that the progression of the overtone ϕ_{21} at long periods is insensitive to the choice of ΔT . The models predict slightly higher ϕ_{21} than actually observed in V440 Per, but the two values are consistent within the error bar.

6 CONCLUSIONS

Using our new Poznań Spectroscopic Telescope we obtained 158 high-precision radial velocity observations of a low-amplitude Cepheid V440 Per. We constructed the pulsation velocity curve of V440 Per and we were able to reliably detect its first harmonic, with an amplitude of only 140 ± 15 m s^{−1}. The measured Fourier phase $\phi_{21} = 2.76 \pm 0.12$ rad differs from the values observed in fundamental-mode Cepheids of a similar period by 7.25σ . Thus, we demonstrated on purely morphological grounds that V440 Per does not pulsate in the fundamental mode. This settles the dispute between Szabó et al. (2007) and Kienzle et al. (1999) and allows us to classify V440 Per as an overtone pulsator, the one with the longest period identified so far ($P = 7.57$ d).

Our results demonstrate that with suitable care, our inexpensive instrument, featuring a MUSICOS Echelle spectrograph and a small robotic telescope, can achieve a stability and precision surpassed only in extrasolar planet searches. Note that we employed neither an iodine cell nor environment control, yet our observations prove that secure mode identification is feasible even for very-low-amplitude Galactic Cepheids.

The overtone pulsation of V440 Per has interesting theoretical consequences. To investigate them we employed our convective linear and non-linear pulsation codes (Smolec & Moskalik 2008). The first-overtone linear models are already constrained by the value of the pulsation period at the centre of the $2\omega_1 = \omega_4$ resonance (Kienzle et al. 1999; Feuchtinger et al. 2000). The very existence of V440 Per imposes additional constraints. Namely, to excite the first overtone linearly and then to obtain a *non-linear full-amplitude* overtone pulsation of such a long period, one has to fine-tune the dynamical convection model used in the pulsation calculations. Our numerical experiments demonstrate that in convective energy transport radiative losses must be properly accounted for to maintain consistency with the observations. With this effect taken into account, non-linear overtone Cepheid models not only reproduce the exceptionally long period of V440 Per, but also reproduce neatly all Fourier parameters of its pulsation velocity curve. No such agreement can be achieved with models pulsating in the fundamental mode. These results from hydrodynamical modelling provide additional support for our empirical classification of V440 Per as a first-overtone pulsator.

ACKNOWLEDGMENTS

Construction of Poznań Spectroscopic Telescope at Adam Mickiewicz University over the course of many years was funded with grants from Polish KBN/MNiSW. Recent work by RB, MF and ASC was supported by MNiSW grant N N203 3020 35. We acknowledge with gratitude permission to use the facilities of – and help from – the Borowiec Geodynamical Observatory of the Centre

for Space Research (CBK PAN, Borowiec), in general, and encouragement from Professor Stanisław Schillak, in particular. RS's and PM's work on the pulsation codes is supported by the MNiSW Grant 1 P03D 011 30. We acknowledge inspiration and support by the late Professor Bohdan Paczynski. Dr Jacques Baudrand kindly supplied us with the blueprints of MUSICOS.

REFERENCES

- Antonello E., Poretti E., Reduzzi L., 1990, *A&A*, 236, 138
 Arellano Ferro A., 1984, *MNRAS*, 209, 481
 Baudrand J., Bohm T., 1992, *A&A*, 259, 711
 Burki G., Benz W., 1982, *A&A*, 115, 30
 Buchler J. R., Moskalik P., Kovács G., 1990, *ApJ*, 351, 617
 Feuchtinger M., 1999, *A&AS*, 136, 217
 Feuchtinger M., Buchler J. R., Kolláth Z., 2000, *ApJ*, 544, 1056
 Gorunya N. A., Irmambetova T. R., Rastorgouev A. S., Samus N. N., 1992, *Pisma Astron. Zh.*, 18, 777
 Gorunya N. A., Samus N. N., Rastorgouev A. S., Sachkov M. E., 1996, *Pisma Astron. Zh.*, 22, 198
 Gorunya N. A., Samus N. N., Sachkov M. E., Rastorgouev A. S., Glushkova E. V., Antipin S. V., 1998, *Pisma Astron. Zh.*, 24, 939
 Grevesse N., Noels A., 1993, in Pratz N., Vangioni-Flam E., Casse M., eds, *Origin and Evolution of the Elements*. Cambridge Univ. Press, Cambridge, p. 15
 Iglesias C. A., Rogers F. J., 1996, *ApJ*, 464, 943
 Kienzle F., Moskalik P., Bersier D., Pont F., 1999, *A&A*, 341, 818
 Kuhfuß R., 1986, *A&A*, 160, 116
 Moskalik P., Kołaczowski Z., 2009, *MNRAS*, 394, 1649
 Moskalik P., Buchler J. R., Marom A., 1992, *ApJ*, 385, 685
 Ogłóza W., Moskalik P., Kanbur S., 2000, in Szabados L., Kurtz D., eds, *ASP Conf. Ser. Vol. 203, The Impact of Large-Scale Surveys on Pulsating Star Research*. Astron. Soc. Pac., San Francisco, p. 235
 Schaller G., Schaerer D., Meynet G., Maeder A., 1992, *A&AS*, 96, 269
 Smolec R., Moskalik P., 2008, *Acta Astron.*, 58, 193
 Soszyński I. et al., 2008, *Acta Astron.*, 58, 153
 Stellingwerf R. F., 1982, *ApJ*, 262, 330
 Szabó R., Buchler J. R., Bartee J., 2007, *ApJ*, 667, 1150
 Wuchterl G., Feuchtinger M. U., 1998, *A&A*, 340, 419
 Yecko P. A., Kolláth Z., Buchler J. R., 1998, *A&A*, 336, 553

APPENDIX A: FOURIER COEFFICIENTS AND THEIR ERRORS

It seems useful to collect in one place all the relevant formulae for Fourier coefficients of velocity $v(t)$ and their errors σ . Defining Fourier series in the following way:

$$\begin{aligned} v(t) - a_0 &= \sum_{n=1}^N A_n \sin(n\omega t + \phi_n) \\ &= \sum_{n=1}^N (a_n \cos n\omega t + b_n \sin n\omega t) \end{aligned} \quad (\text{A1})$$

where N is the order of the fit, we obtain

$$A_n = \sqrt{a_n^2 + b_n^2} \quad \text{and} \quad R_{n1} \equiv \frac{A_n}{A_1}, \quad (\text{A2})$$

$$\tan \phi_n = \frac{a_n}{b_n} \quad \text{and} \quad \phi_{n1} \equiv \phi_n - n\phi_1. \quad (\text{A3})$$

From variations of these equations we find

$$\delta A_n = \frac{a_n \delta a_n + b_n \delta b_n}{A_n}, \quad (\text{A4})$$

$$\delta R_{n1} = R_{n1} \left(\frac{a_n \delta a_n + b_n \delta b_n}{A_n^2} - \frac{a_1 \delta a_1 + b_1 \delta b_1}{A_1^2} \right), \quad (\text{A5})$$

$$\delta \phi_n = \frac{b_n \delta a_n - a_n \delta b_n}{A_n^2}, \quad (\text{A6})$$

$$\delta \phi_{n1} = \frac{b_n \delta a_n - a_n \delta b_n}{A_n^2} - n \frac{b_1 \delta a_1 - a_1 \delta b_1}{A_1^2}, \quad (\text{A7})$$

where the right-hand sides are scalar products of the vector $(\delta a_n, \delta b_n, \delta a_1, \delta b_1) \equiv \delta \mathbf{F}$ and the corresponding derivatives $(\partial/\partial a_n, \partial/\partial b_n, \partial/\partial a_1, \partial/\partial b_1) \equiv \mathbf{L}[\cdot]$. For example, $\delta \phi_{n1} = \mathbf{L}[\phi_{n1}] \cdot \delta \mathbf{F}$ and the third component of vector $\mathbf{L}[\phi_{n1}]$ is $\partial \phi_{n1}/\partial a_1 = -nb_1/A_1^2$. By the law of error propagation, the variance of ϕ_{n1} is

$$\sigma_{\phi_{n1}}^2 \equiv \text{Var}[\phi_{n1}] = \mathbf{L}[\phi_{n1}] \times \mathbf{Cov}[a_n, b_n, a_1, b_1] \times \mathbf{L}[\phi_{n1}]^T, \quad (\text{A8})$$

where $\text{Cov}[\cdot]$ denotes the covariance matrix of raw Fourier coefficients (equation A1), \times denotes matrix multiplication and superscript T indicates the matrix transpose. Analogous expressions hold for other coefficients. The complete linearized transformation matrix \mathbf{M} is obtained by substitution of the \mathbf{L} vectors corresponding to equations (A4)–(A7) as its rows. The full covariance matrix of all Fourier coefficients is seldom needed in practice. It may be obtained from equation (A8) by substitution of \mathbf{M} for \mathbf{L} .

SUPPORTING INFORMATION

Additional Supporting Information may be found in the online version of this article:

Table 1. PST radial velocities of V440 Per.

Please note: Wiley–Blackwell are not responsible for the content or functionality of any supporting information supplied by the authors. Any queries (other than missing material) should be directed to the corresponding author for the article.

This paper has been typeset from a $\text{\TeX}/\text{\LaTeX}$ file prepared by the author.